

AN ANALYSIS OF THE PULSING CHARACTERISTICS OF
THE KANSAS STATE UNIVERSITY TRIGA MARK II NUCLEAR REACTOR

by 503

JERRY W. STAUDER

B.S., Kansas State University, 1967

A MASTER'S THESIS

submitted in partial fulfillment of the

requirements for the degree

MASTER OF SCIENCE

Department of Nuclear Engineering

KANSAS STATE UNIVERSITY

Manhattan, Kansas

1969

Approved by:


Major Professor

LD
2668
74
1969
S 712
C.2

CONTENTS

1.0 INTRODUCTION. 1

2.0 THE TRANSIENT MODEL 3

3.0 REACTOR DESCRIPTION 6

4.0 EXPERIMENTAL DETERMINATION OF THE PARAMETERS. 12

 4.1 Theory 12

 4.2 Experimental Equipment and Procedure 18

 4.3 Results and Discussion 23

5.0 COMPARISON OF TRANSIENT CALCULATIONS WITH TRANSIENT DATA. 32

 5.1 Experimental Equipment and Procedure 32

 5.2 Results and Discussion 34

6.0 SUGGESTIONS FOR FURTHER STUDY 44

7.0 ACKNOWLEDGEMENTS. 46

 LITERATURE CITED. 47

APPENDICES

APPENDIX A: Computer Programs for Average Flux, Centerline
Temperatures, and Average Fuel Temperature
Calculations 49

APPENDIX B: TRIGA Flow Parameters and Temperature Distribution . 64

APPENDIX C: Weighted Least Squares Analysis. 73

APPENDIX D: Solution of the Transient Equations by
Analytic Continuation. 82

APPENDIX E: Average Fuel Heat Capacity 96

APPENDIX F: Thermocouple Temperature Measurement Corrections . . 98

LIST OF FIGURES

1. Elevation view of TRIGA reactor.	7
2. Grid plates.	8
3. TRIGA fuel-moderator element	9
4. Core loading diagram	10
5. TRIGA instrumented fuel element.	15
6. Positioning of the fission chamber in the core	20
7. Fuel and water temperature instrumentation	21
8. Vertical flux distribution in foil insertion holes A, B, C, D, E, and the central thimble.	24
9. Reactor fuel and water temperatures.	26
10. Core thermal conductance as a function of the average fuel temperature.	27
11. Reactivity loss as a function of reactor power	28
12. Reactivity loss as a function of the average fuel temperature rise	29
13. The equipment used to measure the transient power.	33
14. Transient power data and calculations for the \$1.93 pulse.	35
15. Transient power data and calculations for the \$1.76 pulse.	36
16. Transient power data and calculations for the \$1.55 pulse.	37
17. Transient power data and calculations for the \$1.25 pulse.	38
18. Transient temperature data and calculated average fuel temperatures for the \$1.93 pulse	40
19. Transient temperature data and calculated average fuel temperatures for the \$1.76 pulse	41

20.	Transient temperature data and calculated average fuel temperatures for the \$1.55 pulse	42
21.	Transient temperature data and calculated average fuel temperatures for the \$1.25 pulse	43
B-1.	Mass flow rate per ring as a function of reactor power	65
B-2.	Average water temperature rise as a function of reactor power. . .	66
B-3.	Comparison of the calculated power with the measured power	67
B-4.	Film coefficients as a function of reactor power	68
B-5.	Average cladding and average water temperature difference.	69
B-6.	Comparison of the calculated power with the measured power	71
B-7.	Core radial temperature distribution	72
D-1.	Flow sheet of the computer program for the transient calculations.	87
F-1.	Measured and corrected fuel temperatures of the \$1.55 pulse. . . .	101

NOMENCLATURE

a	reactivity insertion rate for the pulse rod going up ($\Delta k/k$ sec)
A_c	cross sectional area of the fuel (cm^2)
A_s	surface area of fueled length of a fuel element (cm^2)
\underline{B}	vector of the solution values
\underline{b}	minimum variance unbiased estimator vector of \underline{B}
$C_i(t)$	precursor density of the i th delayed neutron group at time t (cm^{-3})
$C(\bar{T}_f)$	fuel heat capacity at temperature \bar{T}_f (watt sec/ $^\circ\text{C}$)
C_p	specific heat at constant pressure (watt sec/ $\text{gm } ^\circ\text{C}$)
c	cladding thickness (cm)
\underline{D}	inverse matrix of $\underline{\hat{T}} \underline{V}^{-1} \underline{T}$
\underline{e}	deviation vector
E_f	energy per fission that is released in the fuel (MeV)
\underline{f}	a deviation vector ($\underline{f} = \underline{s}^{-1} \underline{e}$)
g'	reactivity insertion rate for the pulse rod going down ($\Delta k/k$ $^\circ\text{C}$)
g	acceleration of gravity (cm/sec^2)
G	gap thickness (cm)
Gr	Grashoff number
I	number of vertical positions per fuel-moderator element
\underline{I}	identity matrix
k_{eff}	effective multiplication constant
$K(\bar{T}_f)$	core thermal conductance at temperature \bar{T}_f (watts/ $^\circ\text{C}$)
k_f	thermal conductivity of the fuel (watts/cm $^\circ\text{C}$)

k_g	thermal conductivity of the gap (watts/cm °C)
k_c	thermal conductivity of the clad (watts/cm °C)
k	thermal conductivity of the water (watts/cm °C)
\underline{K}	core thermal conductance vector
λ	prompt neutron lifetime (sec)
L	fueled length of a fuel element (cm)
M	total number of fuel elements in the core
m_k	number of fuel elements in the kth ring
\dot{m}	mass flow rate per channel (gms/sec)
$n(t)$	neutron density at time t (cm^{-3})
N_5	U^{235} atom density (nuclei/ cm^3)
Nu	Nusselt number
P	reactor power (watts)
Pr	Prandtl number
q'''	volumetric heat generation rate (watts/ cm^3)
$\overline{q''}$	average volumetric heat generation rate per fuel element (watts/ cm^3)
r_f	radius of the fuel (cm)
R_G	gap resistance (cm °C/watt)
$R_i(t_j)$	remainder term of the Taylor series at time t_j .
\underline{S}	nonsingular symmetric matrix
t	time (sec)
$\bar{T}_f(t)$	average fuel temperature of the core at time t (°C)
\bar{T}_{f0}	average fuel temperature of the core at time zero (°C)
T_{fik}	average radial fuel temperature at the i th level of the k th fuel element (°C)
\bar{T}_{fk}	average temperature of the k th fuel moderator element (°C)

$T(r)$	fuel temperature at radius r ($^{\circ}\text{C}$)
T_{fm}	fuel centerline temperature ($^{\circ}\text{C}$)
T_{w1}	coolant temperature at channel inlet ($^{\circ}\text{C}$)
T_{w2}	coolant temperature at channel outlet ($^{\circ}\text{C}$)
\bar{T}	mixed mean temperature of the coolant ($^{\circ}\text{C}$)
\bar{T}_c	average cladding temperature ($^{\circ}\text{C}$)
\bar{T}_w	average coolant temperature ($^{\circ}\text{C}$)
\underline{T}	temperature matrix
$T_T(t)$	measured fuel temperature at time t ($^{\circ}\text{C}$)
$T_a(t)$	actual fuel temperature at time t ($^{\circ}\text{C}$)
u	unit step function
\underline{V}	variance-covariance matrix of the deviations
$y_i(t_j)$	i th dependent variable at time t_j
$y_i^{(k)}(t_j)$	k th derivative of the i th dependent variable at time t_j
α	reactivity temperature coefficient ($\Delta k/k$ $^{\circ}\text{C}$)
α_1	minimum variance unbiased estimator of the reactivity temperature coefficient
β_i	fraction of delayed neutrons of the i th delayed neutron group
β	total delayed neutron fraction
β	thermal coefficient of volume expansion ($^{\circ}\text{C}^{-1}$)
γ_i	effectiveness of the i th delayed neutron group
$\bar{\gamma}$	average delayed neutron effectiveness
$\Delta\rho_i$	i th reactivity loss
ΔT	temperature difference between average clad and reactor tank bulk water temperature
ϵ	truncation error
λ_i	decay constant of the i th delayed neutron group (sec^{-1})

Λ	prompt neutron generation lifetime (sec)
μ	viscosity of water (gm/sec cm)
$\rho(t)$	reactivity at time t ($\Delta k/k$)
ρ_0	zero power reactivity insertion ($\Delta k/k$)
ρ	density of water (gms/cm ³)
σ_5	fission cross section of U ²³⁵
σ^2	variance
τ_1	time the pulse rod reaches the top of its travel (sec)
τ_2	time the pulse rod drops from its uppermost position (sec)
τ_3	time the pulse rod reaches its lowest position (sec)
τ	time constant (sec)
ϕ_{ik}	average neutron flux at the <i>i</i> th vertical level in the <i>k</i> th fuel element (neutrons/cm ² sec)
ϕ_k	average flux in the <i>k</i> th fuel-moderator element (neutrons/cm ² sec)

1.0 INTRODUCTION .

The pulsing capability of the TRIGA reactor provides a mechanism for research in the areas of dose rate phenomena, short time domain studies, reactor safety and kinetics, and other applications (1,2,3). The development of an analytical model to predict the transient behavior of the TRIGA is necessary in support of pulsed reactor research.

A simplified, space independent approach, known as the Fuchs, or the Fuchs-Nordheim, or the Hansen-Fuchs model (4,5,6,7), which neglects the effects of delayed neutrons and heat transfer, will give a satisfactory description of the reactor power during the prompt burst. However, this model only applies to prompt critical transients where the assumptions of negligible heat transfer and delayed neutron effects will hold.

A more detailed model (4,23) couples the space independent kinetic equations to a space independent thermal model through the reactivity temperature coefficient. This model describes the time dependent behavior for the prompt burst and for later times, when the effects of the delayed neutrons and heat transfer become important. The thermal model is based on an average fuel heat capacity, an average core water heat capacity, a fuel core water resistance, and a core water-reactor tank water resistance.

It is the purpose of this paper to develop a digital code to predict the reactor power and the average fuel temperature of the TRIGA Mark II reactor as functions of time during a transient, and to compare the results with experimental data. A time dependent reactivity input function is developed which describes the net reactivity of the reactor for specific control rod motion and temperature effects. The time dependent position and associated reactivity of the pulse rod are experimentally measured in

this investigation. The thermal model is based on an average fuel heat capacity and a fuel-reactor tank water heat transfer conductance. The heat transfer conductance and the reactivity temperature coefficient needed to complete this model are determined from data obtained in steady state experiments.

The transient model is presented in Section 2.0. Section 4.0 contains the theoretical development, the experimental procedure, and the data from which the heat transfer conductance and the reactivity temperature coefficient were obtained. The comparison between the results of the transient model and the transient data are presented in Section 5.0.

2.0 THE TRANSIENT MODEL

The one energy group, space independent reactor kinetic equations will be used to describe the neutron density. In particular,

$$\frac{dn(t)}{dt} = \frac{\rho(t) - \beta}{\Lambda} n(t) + \sum_i \lambda_i C_i(t), \quad (1)$$

$$\frac{dC_i(t)}{dt} = \frac{\beta_i}{\Lambda} n(t) - \lambda_i C_i(t), \quad i = 1, 2, \dots, 6 \quad (2)$$

where $n(t)$ = neutron density at time t ,

$\rho(t)$ = reactivity at time t ,

Λ = prompt neutron generation lifetime,

β = total delayed neutron fraction,

β_i = fraction of delayed neutrons of the i th delayed neutron group,

λ_i = decay constant of the i th delayed neutron group,

$C_i(t)$ = density of the i th delayed neutron group precursor at time t .

Since delayed neutrons have lower energies than prompt neutrons, they will escape less readily while slowing down, and hence are more effective. This increased effectiveness can be accounted for by substituting a β_{eff} for the experimental value of β (8). In particular,

$$\beta_{\text{eff}} = \bar{\gamma} \beta = \sum_i \gamma_i \beta_i, \quad (3)$$

where $\bar{\gamma}$ is the average delayed neutron effectiveness. A value of β_{eff} is given (9) for the TRIGA Mark II reactor; however, there are no values of γ_i available to correct the i th group fraction. Keepin (10) suggests

that for slow, bare systems,

$$\gamma_i = 1 \quad .$$

A value of the prompt neutron generation time, Λ , is not available for the TRIGA, but a value is given for the prompt neutron lifetime, ℓ (11). These two quantities are related through the effective multiplication constant, k_{eff} , i.e.,

$$\ell = \Lambda k_{\text{eff}} \quad .$$

For most kinetic problems the distinction between Λ and ℓ can be ignored (10). Thus in this work ℓ will be substituted for Λ .

In Eq. (1) the reactivity function must not only describe the initiation of the pulse but also the termination. Thus the following form is assumed,

$$\begin{aligned} \rho(t) = & at - a(t-\tau_1)u(t-\tau_1) - g'(t-\tau_2)u(t-\tau_2) \\ & + g'(t-\tau_3)u(t-\tau_3) - \alpha[\bar{T}_f(t) - \bar{T}_{f0}] \quad , \end{aligned} \quad (4)$$

where a = ramp reactivity insertion rate (pulse rod up),

τ_1 = time the pulse rod reaches the top of its travel,

u = unit step function,

τ_2 = time the pulse rod drops from its uppermost position,

τ_3 = time the pulse rod reaches its lowest position,

g' = ramp reactivity insertion rate (pulse rod down),

α = reactivity temperature coefficient,

$\bar{T}_f(t)$ = average core fuel temperature at time t ,

\bar{T}_{f0} = average core fuel temperature at time zero.

The average fuel temperature can be expressed as

$$C(\bar{T}_f) \frac{d \bar{T}_f(t)}{dt} = P(t) - K(\bar{T}_f) [\bar{T}_f(t) - T_{wl}], \quad (5)$$

where $C(\bar{T}_f)$ = core heat capacity of fuel,

$P(t)$ = reactor power at time t ,

$K(\bar{T}_f)$ = core thermal conductance at average
fuel temperature \bar{T}_f ,

T_{wl} = reactor tank bulk water temperature.

The core thermal conductance is the summation of all the conductances between the fuel and the bulk water temperature. Reactor power is proportional to the neutron flux and thus to the neutron density for a one group approximation, and it can be determined from Eq. (1).

Note in Eqs. (4) and (5) that the coefficients are functions of the average core fuel temperature. Much of the work in this investigation will be devoted to the determination of this average temperature. This is necessary for the calculation of the core thermal conductance and the reactivity temperature coefficient.

3.0 REACTOR DESCRIPTION

The TRIGA reactor core is near the bottom of a tank 20.5 feet deep (see Fig. 1). The tank contains light demineralized water which acts as a coolant, moderator, and radiation shield. The entire reactor assembly is supported by the 1 foot thick graphite reflector assembly which surrounds the core. Upper and lower grid plates bracketed to the reflector provide axial and lateral support for the fuel-moderator elements, the graphite dummy elements, and the control rods. The fuel-moderator elements are cooled by natural convection of the tank water passing down around the outside of the reflector and up through 36 cooling holes in the lower grid plate (see Fig. 2). Triangular-shaped spacers (Fig. 3) on the top-end fixtures of the elements allow the cooling water to pass through the top grid plate (11).

The TRIGA fuel-moderator elements are an alloy of zirconium hydrided to approximately one hydrogen atom for each zirconium atom, and uranium 20% enriched in U^{235} (12). The elements are solid cylinders approximately 1.5 inches in diameter with the fueled region being 14 inches in length. Graphite pieces 4 inches long on either end of the fuel act as upper and lower reflectors. The elements are clad with aluminum 0.030 inches thick. Figure 4 depicts the arrangement of the fuel-moderator elements. Note that the elements form 5 concentric rings, where the innermost ring is designated the B-ring, the next is called the C-ring, and so on out to the F-ring. There are 63 fuel-moderator elements with a total mass of 2291 grams of U^{235} (17).

The reactor is operated with 3 boron carbide control rods. The shim and regulating rods are motor driven and are used for controlling the

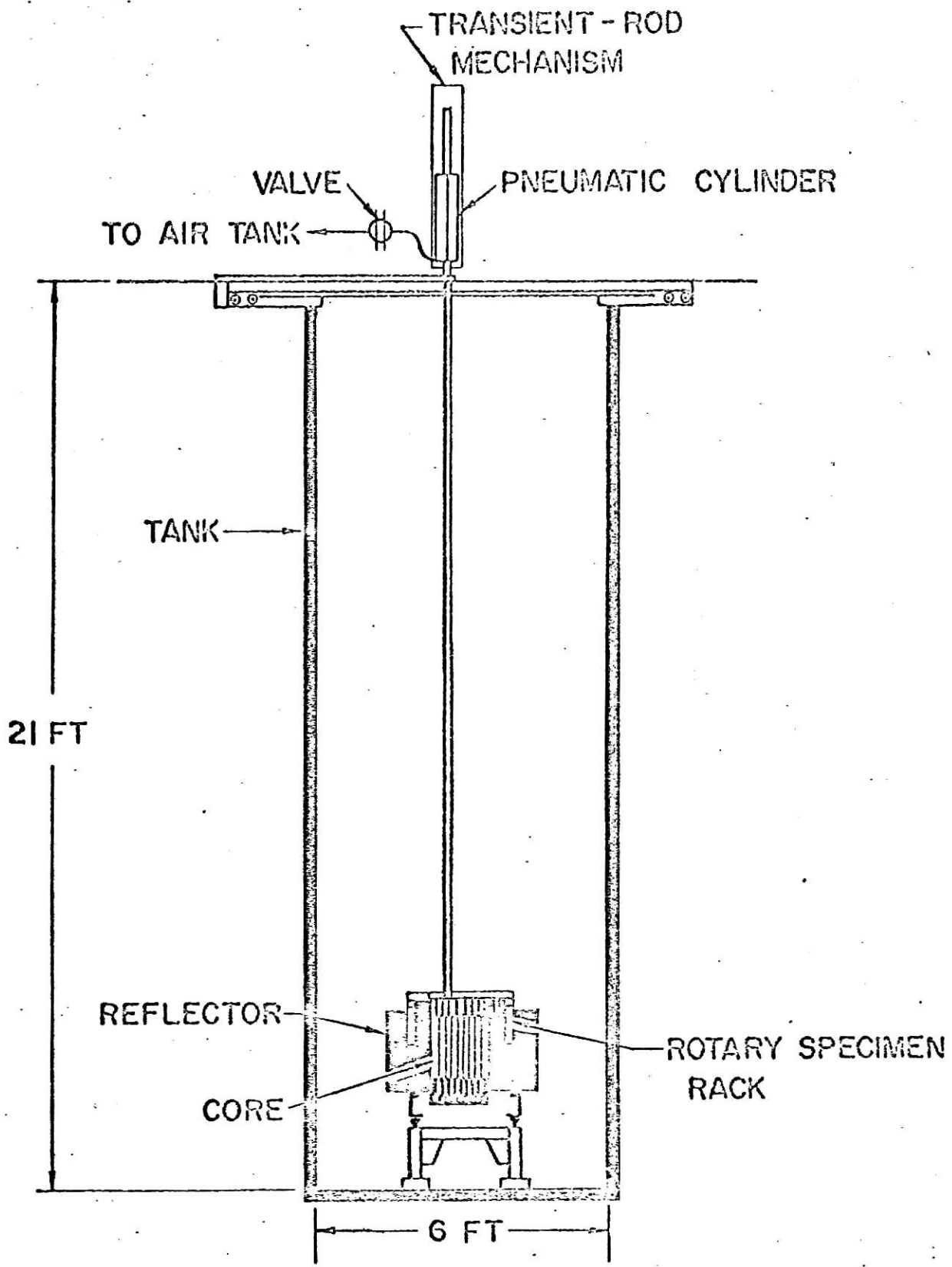


Fig. 1--Elevation view of TRIGA reactor.

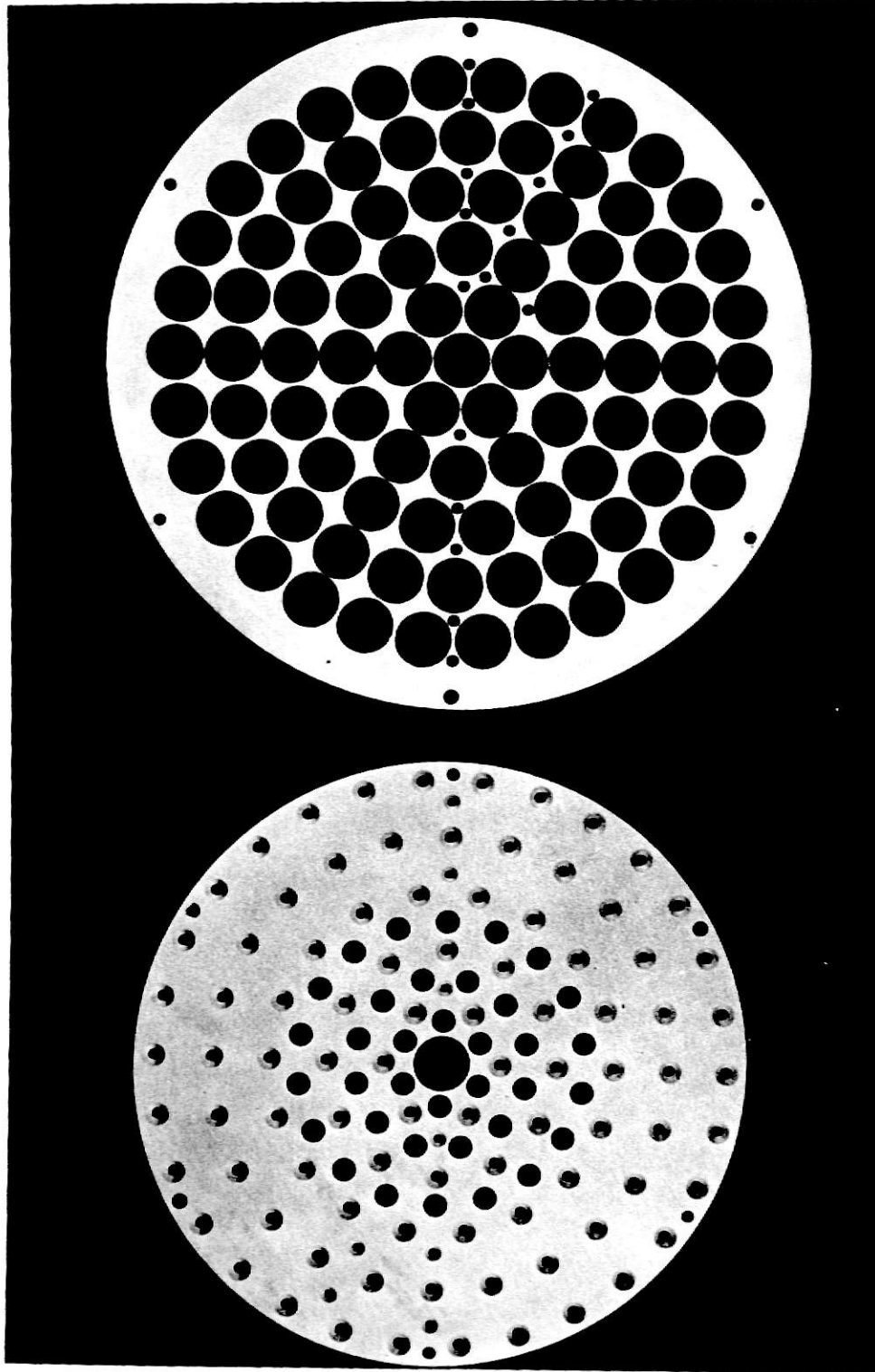


Fig. 2 Grid plates

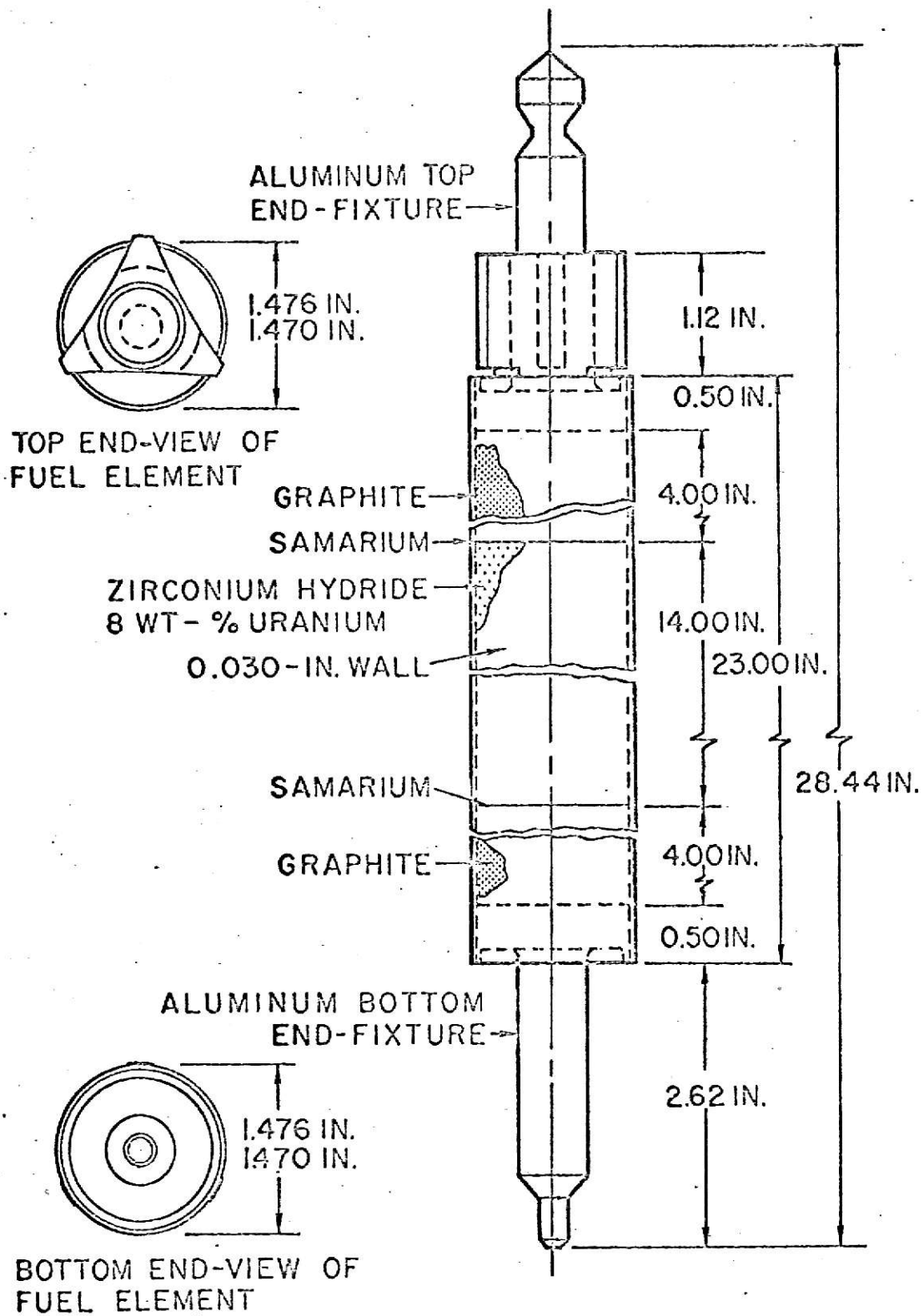


Fig. 3. TRIGA fuel-moderator element.

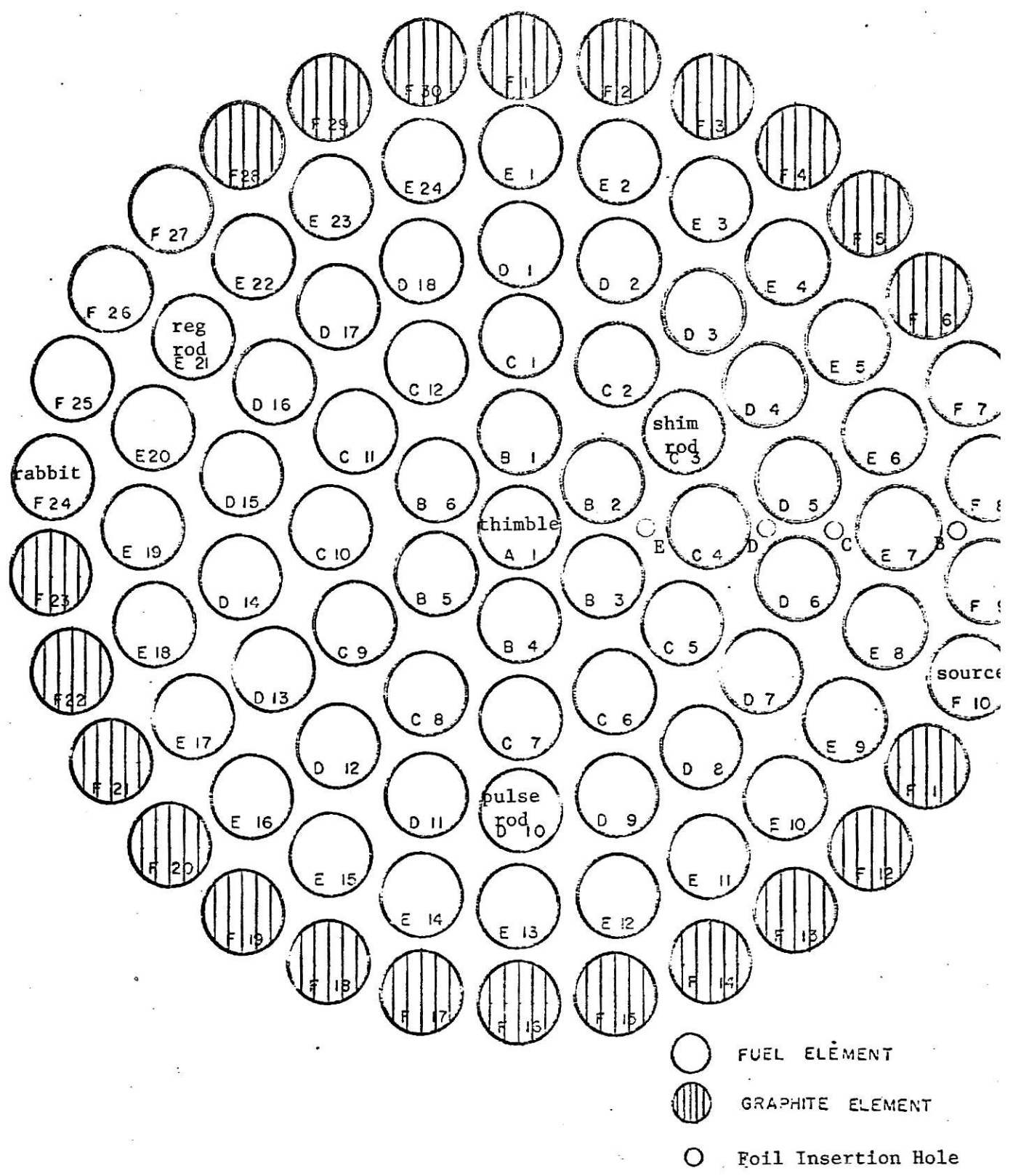


Figure 4. Core-Loading Diagram

power of the reactor. The pulse rod is pneumatically operated and is used for pulsing operations. The pulse rod movement for the KSU TRIGA Mark II reactor is characterized by a finite time interval at the top of its travel. This time interval between the full up position and the start of the drop back into the core is approximately 3 seconds. Thus this time interval (τ_2) has been incorporated into the reactivity input function (Eq. (4)) in addition to the finite travel times (τ_1 and τ_3). Steady state operation is restricted to a reactor power below 250 kilowatts. Transient peak powers are to be held below 250 megawatts.

4.0 EXPERIMENTAL DETERMINATION OF THE PARAMETERS

4.1 Theory

With the reactor at steady state, Eq. (5) becomes

$$P = K(\bar{T}_f) [\bar{T}_f - T_{w1}] ,$$

or

$$K(\bar{T}_f) = \frac{P}{\bar{T}_f - T_{w1}} . \quad (6)$$

Since the power and the average fuel temperature are known, the core thermal conductance can be obtained. The amount of reactivity needed to bring the reactor to a steady state condition at some power is

$$\rho = \rho_0 + \alpha(\bar{T}_f - \bar{T}_{f0}) , \quad (7)$$

where ρ_0 is the zero power reactivity insertion. Zero power is that power where there is negligible heat generation in the fuel. Thus the slope of a curve of ρ vs. $(\bar{T}_f - \bar{T}_{f0})$ will yield the value of the reactivity temperature coefficient.

4.1.1 Average Fuel Temperature

If T_{fik} is the average radial temperature at the i th level in the k th fuel element, then the average temperature of the k th fuel element is

$$\bar{T}_{fk} = \frac{1}{I} \sum_{i=1}^I T_{fik} , \quad (8)$$

where I is the number of vertical positions or levels. The average temperature of the fuel across the core is then

$$\bar{T}_f = \frac{1}{M} \sum_{k=1}^5 m_k \bar{T}_{fk} , \quad (9)$$

where m_k is the number of fuel elements in the k th ring and M is the total number of fuel elements in the core.

4.1.2 Average Radial Temperature

The solution of Poisson's equation for the temperature of the fuel in a long cylindrical fuel element with constant thermal conductivity is

$$T_f(r) = T_{fm} - \frac{q''' r^2}{4 k_f}, \quad (10)$$

where $T_f(r)$ = fuel temperature at radius r ,

T_{fm} = fuel centerline temperature,

q''' = average heat generation rate per unit volume,

k_f = thermal conductivity of the fuel.

The average radial temperature is then

$$T_f = \frac{2}{r_f^2} \int_0^{r_f} T_f(r) r dr = T_{fm} - \frac{q''' r_f^2}{8 k_f}, \quad (11)$$

where r_f is the fuel radius. Thus by measuring the centerline temperature and the heat generation rate, the average radial temperature can be determined.

4.1.3 Heat Generation Rate

In a thermal reactor it may be assumed that 90% of the fission energy is deposited in the fuel elements and that this heat source is distributed in a manner proportional to the neutron flux (8). This heat source is called the volumetric heat generation rate and is expressed in units of power per unit volume. In particular,

$$q''' = E_f N_5 \sigma_5 \bar{\phi}, \quad (12)$$

where E_f = energy per fission that is released in the fuel,
 $N_5 = U^{235}$ atom density,
 σ_5 = fission cross section of U^{235} ,
 $\bar{\phi}$ = average neutron flux.

For the average radial temperature at the i th vertical position of the k th fuel-moderator element (Eq. (11)), the average neutron flux is ϕ_{ik} .

4.1.4 Fuel Centerline Temperature

A TRIGA instrumented fuel-moderator element is presented in Fig. 5. Note that there are only 3 thermocouples and they are located near the middle of the element on its vertical centerline. Thus some estimate must be made of the fuel centerline temperatures at other positions.

The fuel centerline temperature at vertical level z can be expressed as

$$T_{fm}(z) = T_{w1} + \frac{A_c}{\dot{m} c_p} \int_0^z q'''(z) dz \quad (13)$$

$$+ \frac{q'''(z) r_f^2}{2} \left[\frac{1}{2k_f} + \frac{1}{k_G} \ln \left(\frac{r_f + G}{r_f} \right) + \frac{1}{k_c} \ln \left(\frac{r_f + G + c}{r_f + G} \right) + \frac{1}{h(r_f + G + c)} \right],$$

where A_c = cross sectional area of the fuel,

\dot{m} = mass flow rate of coolant in channel surrounding the fuel-moderator element,

c_p = specific heat at constant pressure of coolant,

k_G = thermal conductivity of the gap,

G = gap thickness,

k_c = thermal conductivity of the cladding,

c = cladding thickness,

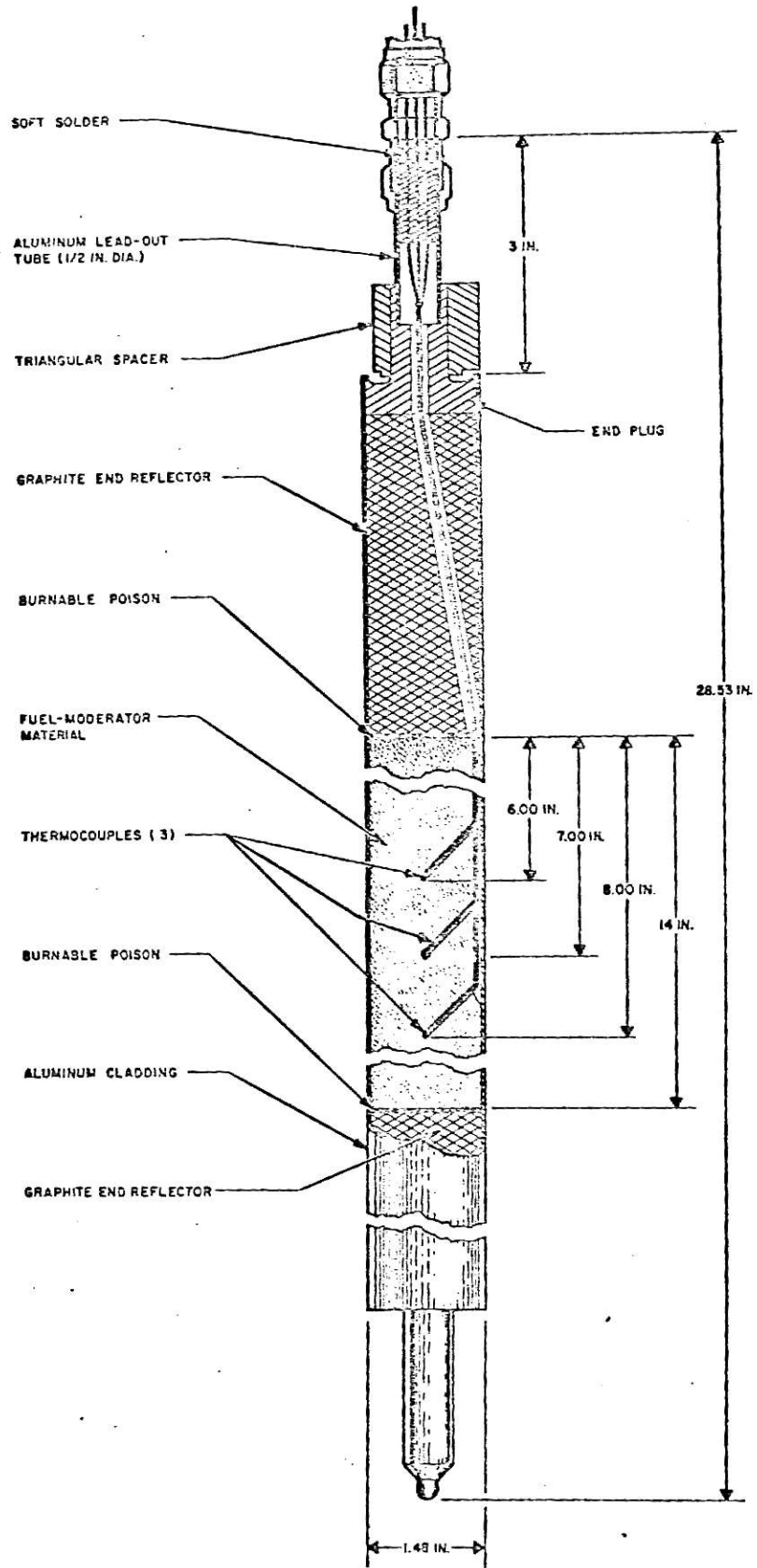


Figure 5. TRIGA instrumented fuel element

h = film coefficient of heat transfer between the fuel moderator element and the coolant,

T_{w1} = coolant temperature at channel inlet.

The lower limit on the integration of the heat generation rate starts at the bottom of the active region of the fuel element.

All of the above quantities are known or can be measured except the film coefficient h , the flow rate \dot{m} , the thermal conductivity of the gap k_G , and the thickness of the gap G . Bonilla (13) suggests the use of the following correlation for natural convection flow past vertical tubes,

$$Nu = 0.13 (GrPr)^{1/3}, \quad (14)$$

where Nu , Gr , and Pr are the Nusselt, Grashoff, and Prandtl numbers respectively. Recall that

$$Nu = h L/k,$$

where L is length of the active portion of the fuel-moderator element, and k is the thermal conductivity of the coolant. The Grashoff number is defined as

$$Gr = \rho^2 L^2 g \beta \Delta T / \mu^2,$$

where ρ , β , and μ are the density, thermal coefficient of volume expansion, and the viscosity of the coolant respectively. The temperature difference, ΔT , used was the difference between the average cladding and the reactor tank bulk water temperature, i.e., $\bar{T}_c - T_{w1}$. The Prandtl number is defined as

$$Pr = c_p \mu / k.$$

The physical properties of the coolant are evaluated at the mixed mean temperature, i.e.,

$$\bar{T} = (\bar{T}_c + \bar{T}_w)/2, \quad (15)$$

where \bar{T}_c = the average cladding temperature,

\bar{T}_w = the average coolant temperature (the arithmetic mean of the channel inlet and outlet water temperatures).

The average cladding temperature is determined by

$$\bar{T}_c = \bar{T} + \frac{r_f^2 \bar{q}'''}{2(r_f + G + c)h} \quad (16)$$

where \bar{q}''' is the average heat generation rate in the fuel-moderator element.

The mass flow rate of the coolant can be found by making a heat balance between the fuel element and the cooling water. In particular,

$$\dot{m} = \frac{A_c}{c_p (T_{w2} - T_{w1})} \int_0^L q'''(z) dz, \quad (17)$$

where T_{w2} is the channel outlet temperature.

Making the substitution,

$$R_G = \frac{1}{k_G} \ln \left(\frac{r_f + G}{r_f} \right),$$

into Eq. (13) and rearranging leads to

$$R_G = \frac{T_{fm}(z) - T_{w1} - \frac{A_c}{\dot{m} c_p} \int_0^z q'''(z) dz}{q'''(z) r_f^2} \quad (18)$$

$$- \left(\frac{1}{4k_f} + \frac{1}{2k_c} \ln \left(\frac{r_f + c}{r_f} \right) + \frac{1}{2(r_f + c)h} \right),$$

where the gap thickness has been assumed to be negligibly small.

The procedure to estimate the centerline temperature along the k th fuel-moderator element is as follows:

1. Assume an average cladding temperature and calculate the mixed mean temperature of the coolant using Eq. (15).
2. Estimate the film coefficient by Eq. (14).
3. Check the assumed \bar{T}_c by Eq. (16) and if not within a specified accuracy, repeat steps 1, 2, and 3 with the new \bar{T}_c .
4. When the preceding steps have been completed satisfactorily, calculate the gap conductance by Eq. (18) for the three measured centerline temperatures and average linearly.
5. Estimates of the centerline temperatures can now be made at any vertical position with Eq. (13) using the average gap conductance and the film coefficient.

4.2 Experimental Equipment and Procedure

4.2.1 Absolute Flux Measurements

The spatial neutron flux distribution in the core was measured with a 0.025 inch outside diameter fission chamber made by Reuter-Stokes Electronics Components, Inc. of Cleveland, Ohio. The chamber was inserted into the core through the 0.314 inch foil insertion holes in the upper grid plate. See Fig. 4 for the location of these holes.

The thermal neutron operating range of the detector is from 1×10^8 to 2×10^{14} neutrons/cm² sec. The active length of the detector is 1 inch and the sensitive volume is 0.1 cm³ which contains He gas at 76 cm Hg.

The outer shell is 304 stainless steel, the inner electrode Titanium, and the neutron absorber is U_3O_8 enriched 93% in U^{235} and containing 3.34 milligrams of U^{235} (14). The U_3O_8 thickness is 1 milligram/cm² and the plated area is 4.08 cm². Twenty feet of coaxial cable is provided with the chamber.

Figure 6 shows the fission chamber and associated equipment as used to map the flux in the core. The chamber and cable were housed in a flexible aluminum tube filled with water, but the 26 11/16 inch aluminum probe at the bottom is rigid and it positioned the chamber in the core. All the equipment except the chamber was located on top of the reactor shield.

From its bottom-most position the chamber was withdrawn at a rate of 1 inch per minute and readings were taken at 0.5 inch intervals. Since its lowest position was fixed with respect to the upper grid plate, the position of the fission chamber was always known.

4.2.2 Fuel and Water Temperature Measurements

Figure 7 shows the instrumentation used to measure the fuel and water temperatures. The thermocouples are chromel-alumel and a Leeds-Northrup potentiometer was used to measure their emf.

The instrumented fuel element normally in B-3, number 2788 E-TC, was used to make all the fuel temperature measurements. With the series of measurements completed with the element in B-3, it was exchanged with the element in C-4 and the measurements repeated. This same procedure was followed for the elements in D-6, E-7, and F-8.

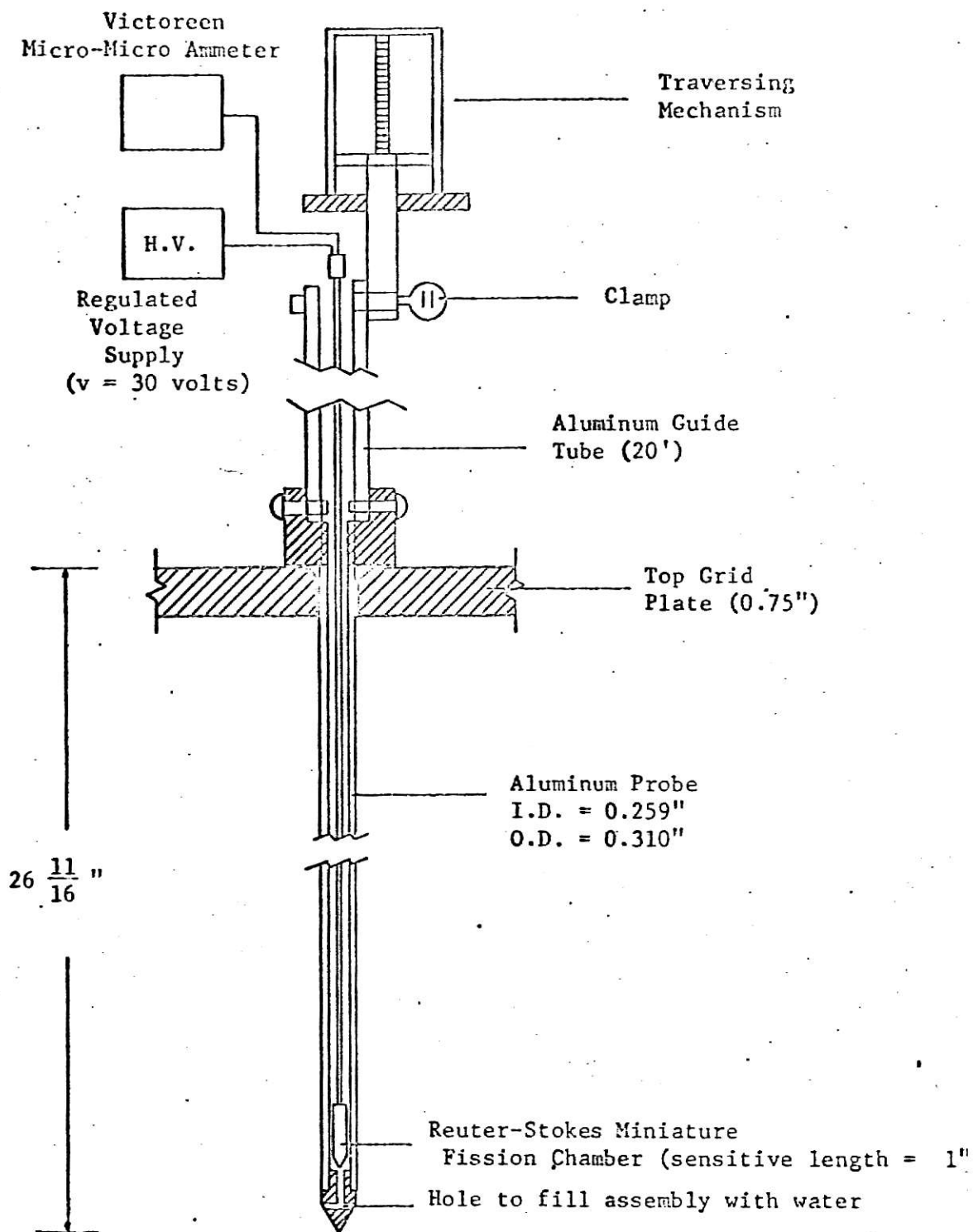


Figure 6. Positioning of the fission chamber in the core

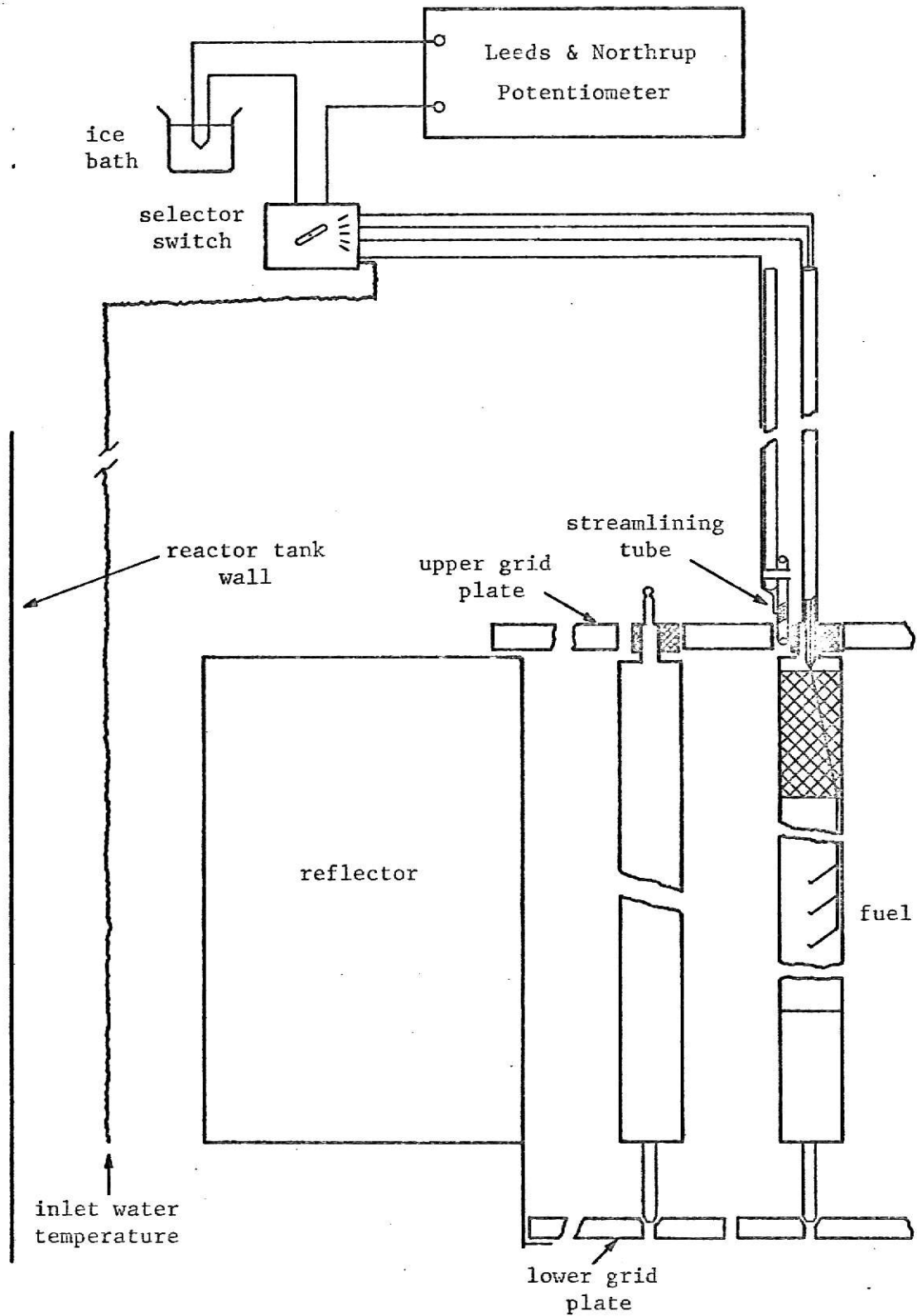


Figure 7. Fuel and water temperature instrumentation. (Note that this thermocouple circuit is not recommended for accurate measurements. See Leeds and Northrup recommended circuits.)

The thermocouple, which measured the exit water temperature from the channel which surrounds the instrumented fuel element, was placed in a streamlining tube to reduce the turbulence of the water. It was found through earlier measurements that without the streamlining tube it was very difficult to obtain a steady reading because of the turbulence of the water surrounding the thermocouple. The streamlining tube with the thermocouple was placed into the space between the triangular block and the grid plate with a long flexible aluminum tube.

A thermocouple was placed in the water about halfway between the reflector and the reactor tank wall and approximately level with the bottom of the reflector. This measurement was considered to be the inlet water temperature to the core.

The series of measurements with the instrumented fuel-moderator element in each ring consisted of the 3 fuel temperatures, and the inlet and outlet water temperatures across the fuel element, all taken at various steady state power levels from zero power to 250 kW.

4.2.3 Reactivity Measurements

For each steady state power level where the fuel and water temperatures were recorded, the critical position was also recorded, i.e., the shim and regulating rod positions. Prior to these measurements, the rods were calibrated by the procedure outlined in the KSU Hazards Summary Report (11).